

Silver as a highly effective bonding layer for lead telluride thermoelectric modules assembled by rapid hot-pressing



C. C. Li ^{a,b}, F. Drymiotis ^b, L. L. Liao ^c, M. J. Dai ^c, C. K. Liu ^c, C. L. Chen ^d, Y. Y. Chen ^d, C. R. Kao ^{a,*}, G. J. Snyder ^{b,*}

^a Department of Materials Science & Engineering, National Taiwan University, Taipei, Taiwan

^b Materials Science, California Institute of Technology, Pasadena, CA, USA

^c Electronic and Optoelectronics Research Laboratories, Industrial Technology Research Institute, Hsinchu, Taiwan

^d Institute of Physics, Academia Sinica, Taipei, Taiwan

ARTICLE INFO

Article history:

Received 19 August 2014

Accepted 23 March 2015

Keywords:

Rapid hot-pressing

Thermoelectric material

Intermetallic compounds

Thermal stability

ABSTRACT

We use the rapid hot-pressing method to bond Ag foil onto pure PbTe in order to assess its effectiveness as a bonding layer material for thermoelectric module applications. Scanning electron microscopy and X-ray diffraction are employed to examine intermetallic compound formation and microstructure evolution during isothermal aging at 400 °C and 550 °C. We find that Ag is a promising bonding material for PbTe modules operating at $T_{\text{Hot}} \leq 400$ °C. Additionally, our approach highlights a highly effective and inexpensive method to metallize PbTe prior to module assembly.

© 2015 Elsevier Ltd. All rights reserved.

1. Introduction

Thermoelectric power generation, based on the Seebeck effect, is renewable and has negligible carbon footprint. Consequently it has attracted an increasing amount of attention. Thermoelectric power generation modules designed to convert industrial or automotive waste heat into electrical energy, can provide a sizable energy output from the waste heat. Hence, high-efficiency bulk thermoelectric materials have been intensively developed worldwide over the past decade. For some of these materials the dimensionless thermoelectric figure of merit (zT), approaches $zT \sim 2$, which can translate to 20% of Carnot efficiency when incorporated into a device [1,2]. Even though significant progress has been attained in the development of high efficiency thermoelectric compounds, the development of thermoelectric modules to take advantage of these materials has not been as rapid. So far, only low-temperature (<200 °C) thermoelectric materials, such as Bi_2Te_3 -based alloys, have been widely developed and incorporated in commercial cooling or heating devices [3–6]. Mid-temperature (200–600 °C) PbTe-based thermoelectric devices assembled by high temperature fabrication processes, such as brazing or diffusion bonding, have lower yields and fierce diffusion problems that

degrade thermoelectric performance and show poor adhesion during long-term service [7–10]. A similar situation exists in the case of CoSb_3 -based thermoelectric devices [11].

The use of a bonding layer, inserted between the thermoelectric component and the electrode, is needed for low electrical and thermal contact resistance. The objective of this study is to develop appropriate bonding materials that will allow reliable long-term operation in PbTe-based thermoelectric modules [12–14]. According to the vertical section of the AgPbTe ternary phase diagram [15], Ag could react with PbTe to form Ag_2Te intermetallic compound. Many recent works have reported the good thermoelectric properties of Ag_2Te itself, and furthermore, Ag also enhances the performance of PbTe [16–20]. Silver is known to be soluble in PbTe with significant temperature dependence. This temperature dependence of Ag, in metal rich PbTe results in n-type doping from interstitial Ag, which leads to a temperature dependence of the n-type dopant concentration. In Te rich p-type samples, the Ag likely fills Pb vacancies, donating electrons, but also replaces some additional Pb acting as acceptor, as well as donating electrons when Ag goes to interstitial positions [18,21]. Additionally, the coefficient of thermal expansion (CTE) of Ag is $18.9 \times 10^{-6}/\text{K}$, very close to that of PbTe ($20.4 \times 10^{-6}/\text{K}$) [22,23]. This small difference will reduce potential reliability issues arising from the CTE mismatch. Hence, Ag is chosen as the bonding material in this work because of its good electrical and thermal conductivity, and low CTE mismatch. Issues relating to the identification of intermetallic compounds, microstructure evolution during mid-temperature operation and

* Corresponding authors. Tel.: +886 2 33663745 (C.R. Kao), +1 626 395 6220 (G.J. Snyder).

E-mail addresses: crkao@ntu.edu.tw (C.R. Kao), jsnyder@caltech.edu (G.J. Snyder).

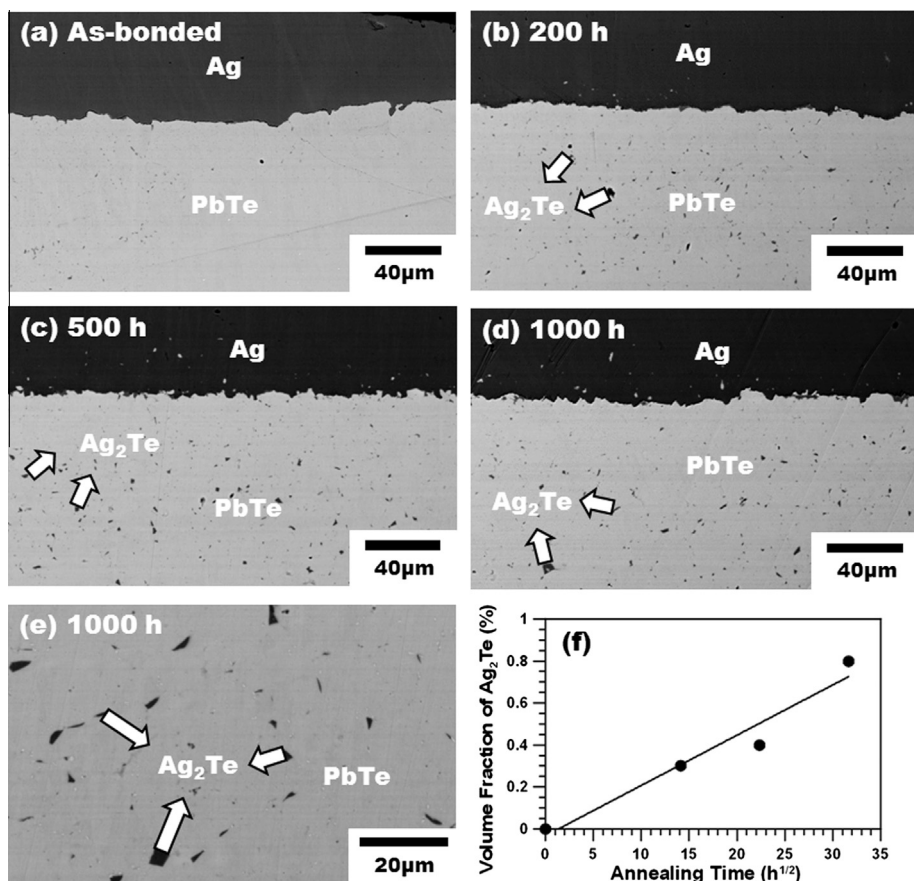


Fig. 1. Interfaces of Ag/PbTe/Ag after aging at 400 °C for (a) 0, (b) 200, (c) 500 and (d) 1000 h. (e) Zoom-in view for the PbTe region of (d). (f) Volume fraction of Ag₂Te as a function of square root of the annealing time.

thermoelectric behavior will be also be discussed. This work should provide the foundation for building thermoelectric modules for power generating which require long-term operations at high temperature.

2. Experimental

In this study, stoichiometric PbTe ingots were prepared by melting Pb (99.999%) and Te (99.999%) in an evacuated and sealed quartz tube at 1000 °C for 6 h, followed by annealing at 700 °C for 48 h to ensure the homogeneity. The resulting PbTe ingots were then ground into powders by ball milling in Ar atmosphere for 1 h. The mean particle size (diameter) of PbTe powders after milling was $8.5 \pm 2.1 \mu\text{m}$. Silver foil (99.9%) with a thickness of 127 μm was polished using an 800 grit SiC sandpaper and then cleaned with acetone in an ultrasonic bath. After the Ag foil had been cleaned, 4 g of PbTe powder were placed between two polished Ag foils inside a graphite die to produce a disk 3 mm thick with diameter of 12 mm. The resulting Ag/PbTe/Ag structure was subsequently placed in a hot press, in which it was bonded and sintered for 3 h under Ar flow. The bonding pressure and temperature were 40 MPa and 550 °C, respectively. Finally, the samples were retrieved and isothermally annealed at 400 °C and 550 °C. Following each annealing process, the samples were mounted in epoxy resin, and metallurgically polished. The Seebeck coefficient [24], and thermal diffusivity (Netzsch LFA 457) were measured along the pressing direction as appropriate for its intended use. The thermal conductivity for each sample was calculated using the relation $\kappa = DdC_p$, with D being the measured diffusivity, d the sample density, and C_p the heat capacity at constant pressure. The density used in the calculation was the measured density at

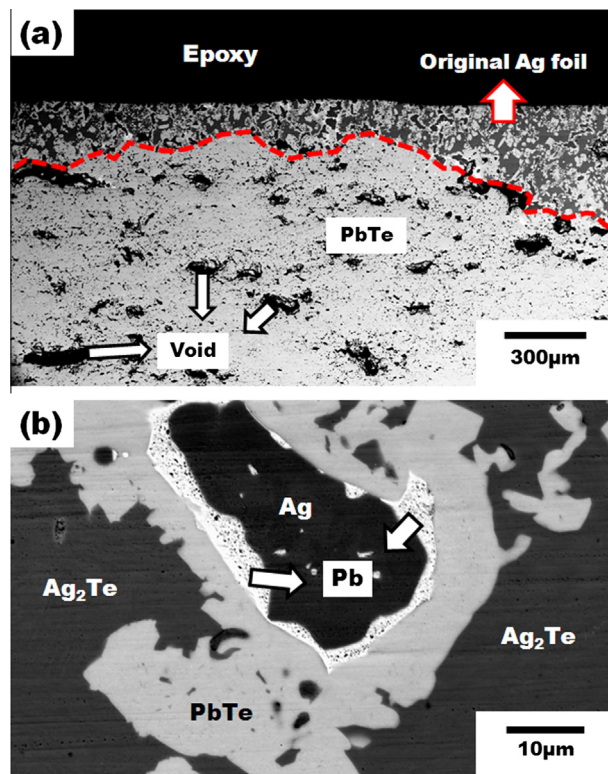


Fig. 2. Micrographs of Ag/PbTe/Ag after aging at 550 °C for 50 h. (a) Low magnification view showing the Ag foil had disappeared. (b) Zoom-in view showing the co-existence of the reactants and the reaction products.

room temperature, and the value of C_p was taken to be the value of the Dulong–Petit limit.

3. Results and discussion

The microstructure evolution of the Ag/PbTe/Ag structures after annealing at 400 °C is shown in Fig. 1. As shown in Fig. 1(a), a nearly perfect Ag/PbTe interface is observed after bonding. The interface is uniform and without cracks. As aging time increases, the interface remains stable, even after 1000 h of aging, but more and more black particles appear and distribute uniformly within PbTe, as shown in Fig. 1(b)–(d). A zoom-in view of these black particles is shown in Fig. 1(e). These particles turn out to be Ag_2Te according to Energy Dispersive X-ray Spectroscopy (EDS) analysis. When the annealing time reaches 1000 h, the solubility of Ag in PbTe matrix is about 1.7 ± 0.2 at.%. To determine the amounts of Ag_2Te particles we used the technique of quantitative metallography. This technique estimates the volume fraction of a certain phase by measuring the area fraction occupied by this phase in a two-dimensional cross section [25]. Several samples were cross-sectioned and imaged at five random locations for each aging time.

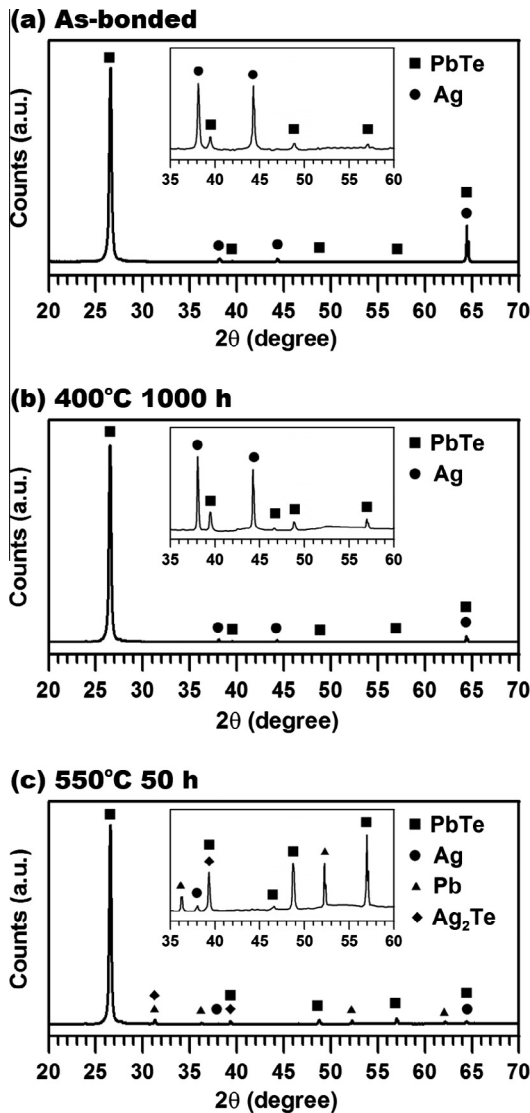


Fig. 3. X-ray diffraction patterns of (a) as-bonded Ag/PbTe/Ag, (b) Ag/PbTe/Ag aged at 400 °C for 1000 h, and (c) Ag/PbTe/Ag aged at 550 °C for 50 h. The inset in each figure is the zoom-in for those peaks between 35° and 60°.

For annealing times of 200, 500, and 1000 h, the Ag_2Te volume fraction was estimated to be 0.3%, 0.4% and 0.8% respectively. The Ag_2Te volume fraction is plotted versus the square root of annealing time in Fig. 1(f). As can be seen here the amount of Ag_2Te increases following parabolic kinetics, which suggests that the formation of this phase is a diffusion-limited process. It is proposed that the diffusion of Ag through PbTe is the rate-limiting step. From this kinetic data, the double-sided 127 μm Ag foils will be consumed after annealing at 400 °C for 38 years. This time frame is far beyond the expected lifetime of typical thermoelectric devices.

While the interface is highly stable at 400 °C for a very long period of time, an upper temperature limit does exist for such an interface. Fig. 2 shows the microstructure evolution of Ag/PbTe/Ag after annealing at 550 °C for 50 h. The Ag foils reacted vigorously with PbTe to form Ag_2Te , according to the following reaction:



After 50 h, both the upper and the lower Ag foils have disappeared, as shown in Fig. 2(a). The region above the dashed curve in Fig. 2(a) experiences the most severe reaction, while the region below the dashed curve still contains un-reacted bulk PbTe. Fig. 2(b) shows a zoom-in view of the upper region, which shows the presence of unreacted Ag and PbTe. It should be noted that 550 °C is higher than the melting temperature of Pb (327.5 °C). Hence, Pb is in the liquid state during annealing and can easily flow through the PbTe matrix, causing the formation of large voids.

Fig. 3 shows the X-ray diffraction patterns of the as-bonded Ag/PbTe/Ag and after annealing. In the as-bonded condition, the peaks of PbTe and Ag can be easily identified, as shown in

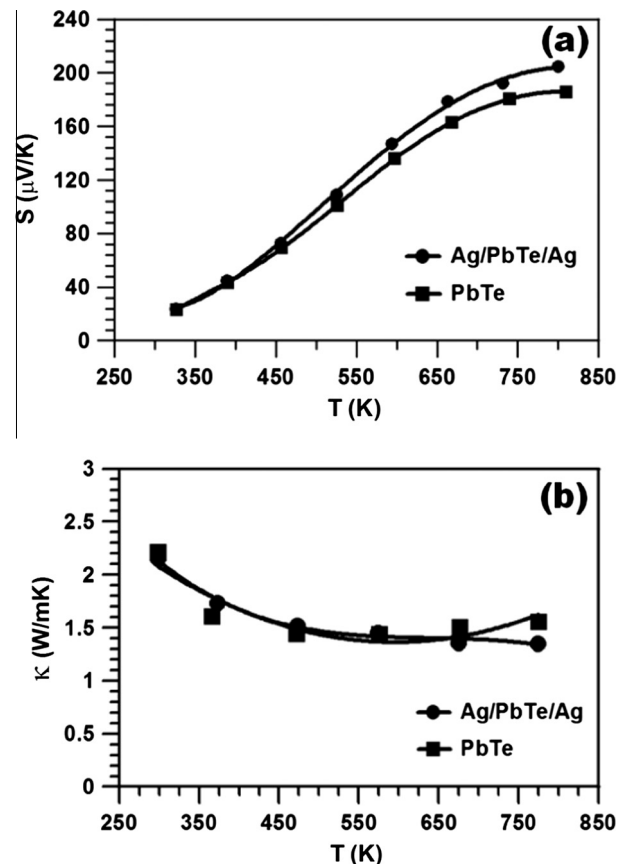


Fig. 4. (a) Seebeck coefficients and (b) thermal conductivities of pure PbTe and Ag/PbTe/Ag from 300 to 823 K.

Fig. 3(a). After annealing at 400 °C for 1000 h, only peaks from PbTe and Ag are identified since the amount of Ag₂Te is below the detection limit (0.8% volume fraction), as shown in Fig. 3(b). After annealing at 550 °C for 50 h, as shown in Fig. 3(c), peaks from PbTe, Ag, Pb, and Ag₂Te can be identified. The pattern is consistent with the microstructure observation shown in Fig. 2.

In Fig. 4(a) we show the Seebeck coefficient (*S*) of the stoichiometric PbTe and the Ag/PbTe/Ag structure obtained in the temperature range 300–823 K. Both samples exhibit p-type behavior within the entire range of measurement. The Seebeck coefficients of both samples gradually increase to a maximum at approximately 800 K. The Seebeck coefficient of Ag/PbTe/Ag is slightly higher than that of pure PbTe in the entire temperature range, which is consistent with a slightly lower p-type carrier concentration. Fig. 4(b) shows the thermal conductivity as a function of temperature for both samples. The thermal conductivity for both samples is in good agreement at low temperatures until the temperature reached 675 K. Above that temperature we observe an increase in the thermal conductivity of stoichiometric PbTe, which is presumably due to bipolar contribution.

4. Conclusion

We conclude that Ag is an effective bonding layer for PbTe based modules, designed to operate at $T \leq 400$ °C. The interface between Ag and PbTe remains uniform and without cracks even after extended annealing. We do observe the formation of Ag₂Te precipitates at 400 °C within the PbTe matrix, but the Ag₂Te showed no inclination to aggregate at the interface. Furthermore, the coefficient of thermal expansion of Ag ($18.9 \times 10^{-6}/\text{K}$) is very close to that of PbTe ($20.4 \times 10^{-6}/\text{K}$), which will greatly decrease the shear stress present at the interface. One aspect that merits further investigation is the distribution of the Ag₂Te precipitates within the PbTe matrix. More than likely, the Ag₂Te precipitates are not distributed uniformly, which may lead to variations in the Seebeck coefficient and electrical conductivity due to local changes in stoichiometry. This has been observed for example in the case of $(\text{AgSbTe}_2)_x(\text{PbTe})_{1-x}$ [26]. Scanning Seebeck measurements will be required in order to properly assess the effect of the precipitates on thermoelectric performance and determine the proper p and n doping in order to nullify their effect and consequently optimize thermoelectric performance. Regardless, our initial results suggest that Ag is a promising bonding layer material for PbTe-based thermoelectric modules.

Acknowledgements

This work is financially supported by National Science Council of Taiwan through Grant 101-2221-E-002-162-MY3, the Electronics and Optoelectronics Research Laboratories of Industrial Technology Research Institute, and the Caltech DOW-Bridge program.

References

- [1] Biswas K, He J, Blum ID, Wu CI, Hogan TP, Seidman DN, et al. High-performance bulk thermoelectrics with all-scale hierarchical architectures. *Nature* 2012;489:414–8.
- [2] Pei Y, Wang H, Snyder GJ. Band engineering of thermoelectric materials. *Adv Mater* 2012;24:6125–35.
- [3] Karri MA, Thacher EF, Helenbrook BT. Exhaust energy conversion by thermoelectric generator: two case studies. *Energy Convers Manage* 2011;52:1596–611.
- [4] Karabetoglu S, Sisman A, Ozturk ZF, Sahin T. Characterization of a thermoelectric generator at low temperatures. *Energy Convers Manage* 2012;62:47–50.
- [5] Li CC, Zhu ZX, Liao LL, Dai MJ, Liu CK, Kao CR. Assembly of N type Bi₂(Te, Se)₃ thermoelectric modules by low temperature bonding. *Sci Technol Weld Joining* 2013;18:421–4.
- [6] Lesage FJ, Pelletier R, Fournier L, Sempels ÉV. Optimal electrical load for peak power of a thermoelectric module with a solar electric application. *Energy Convers Manage* 2013;74:51–9.
- [7] Xia H, Drymiotis F, Chen CL, Wu A, Snyder GJ. Bonding and interfacial reaction between Ni foil and n-type PbTe thermoelectric materials for thermoelectric module applications. *J Mater Sci* 2014;49:1716–23.
- [8] Wojciechowski KT, Zybala R, Mania R. High temperature CoSb₃–Cu junctions. *Microelectron Reliab* 2011;51:1198–202.
- [9] Weinstein M, Mlavsky AI. Bonding of lead telluride to pure iron electrodes. *Rev Sci Instrum* 1962;33:1119–20.
- [10] Zhao D, Geng H. Microstructure contact studies for Skutterudite thermoelectric devices. *Int J Appl Ceram Technol* 2012;9:733–41.
- [11] Zhao D, Li X, He L, Jiang W, Chen L. Interfacial evolution behavior and reliability evaluation of CoSb₃/Ti/Mo–Cu thermoelectric joints during accelerated thermal aging. *J Alloy Compd* 2009;477:425–31.
- [12] Hadjistassou C, Kyriakides E, Georgiou J. Designing high efficiency segmented thermoelectric generators. *Energy Convers Manage* 2013;66:165–72.
- [13] Snyder GJ, Toberer ES. Complex thermoelectric materials. *Nat Mater* 2008;7:105–14.
- [14] Fraisse G, Ramousse J, Sgorlon D, Goupil C. Comparison of different modeling approaches for thermoelectric elements. *Energy Convers Manage* 2013;65:351–6.
- [15] Grieb B, Lugscheider E, Wilden J. Silver–Lead–Tellurium, Ternary Alloys, vol. 2. VCH; 1988. p. 465–476.
- [16] Pei YZ, Lensch-Falk J, Toberer ES, Medlin DL, Snyder GJ. High thermoelectric performance in PbTe due to large nanoscale Ag₂Te precipitates and La doping. *Adv Funct Mater* 2011;21:241–9.
- [17] Urban JJ, Talapin DV, Shevchenko EV, Kagan CR, Murray CB. Synergism in binary nanocrystal superlattices leads to enhanced p-type conductivity in self-assembled PbTe/Ag₂Te thin films. *Nat Mater* 2007;6:115–21.
- [18] Pei Y, May A, Snyder G. Self-tuning the carrier concentration of PbTe/Ag₂Te composites with excess Ag for high thermoelectric performance. *Adv Energy Mater* 2011;1:291–6.
- [19] Drymiotis F, Day TW, Brown DR, Heinz NA, Snyder GJ. Enhanced thermoelectric performance in the very low thermal conductivity Ag₂Se_{0.5}Te_{0.5}. *Appl Phys Lett* 2013;103:143906.
- [20] Pei Y, Heinz NA, LaLonde A, Snyder GJ. Combination of large nanostructures and complex band structure for high performance thermoelectric lead telluride. *Energy Environ Sci* 2011;4:3640–5.
- [21] Bergum K, Ikeda T, Snyder GJ. Solubility and microstructure in the pseudo-binary PbTe–Ag₂Te system. *J Solid State Chem* 2011;184:2543–52.
- [22] Lide DR. *CRC Handbook of Chemistry and Physics*. 84th ed. Boca Raton (Florida): CRC Press; 2003.
- [23] Houston B, Strakna RE, Belson HS. Elastic constants, thermal expansion, and Debye temperature of lead telluride. *J Appl Phys* 1968;39:3913–7.
- [24] Iwanaga S, Toberer ES, Lalonde A, Snyder GJ. A high temperature apparatus for measurement of the Seebeck coefficient. *Rev Sci Instrum* 2011;82:063905.
- [25] Voort GFV. *ASM Handbook: Metallography and Microstructures*. Materials Park (OH): ASM International; 1985.
- [26] Chen N, Gascoin F, Snyder GJ, Muller E, Karpinski G, Stiewe C. Macroscopic thermoelectric inhomogeneities in $(\text{AgSbTe}_2)_x(\text{PbTe})_{1-x}$. *Appl Phys Lett* 2005;87:171903.